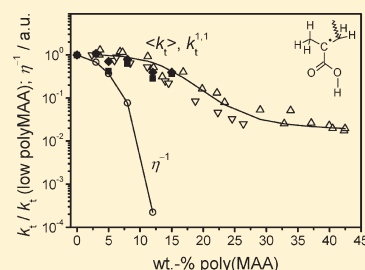


SP-PLP-EPR Study into the Termination Kinetics of Methacrylic Acid Radical Polymerization in Aqueous Solution

Johannes Barth and Michael Buback*

Institute for Physical Chemistry, University of Göttingen, Tammannstrasse 6, D-37077 Göttingen, Germany

ABSTRACT: The termination kinetics of methacrylic acid (MAA) radical polymerization in aqueous solution containing 10 wt % MAA was measured via the single pulse—pulsed laser polymerization—electron paramagnetic resonance (SP-PLP-EPR) method from 0 to 50 °C. The termination rate coefficient, k_t , was determined as a function of radical chain length. Addition of high-molecular-mass poly(methacrylic acid), which mimicks monomer conversion, leads to a reduction of k_t , which is however far below the associated decrease in fluidity, η^{-1} .



INTRODUCTION

Radical polymerization in aqueous solution is of both academic and of industrial interest. The detailed mechanistic understanding and the availability of accurate rate coefficients for the individual reaction steps are thus highly desirable. So far, propagation in aqueous-phase radical polymerization has been thoroughly studied by the pulsed laser polymerization—size exclusion chromatography (PLP-SEC) technique,^{1–7} which is the IUPAC-recommended method for reliable measurement of propagation rate coefficients, k_p .⁸ Toward lower monomer concentration, k_p is significantly enhanced, typically by 1 order of magnitude in passing from bulk polymerization to reaction in dilute aqueous solution. No such changes are found for propagation of common monomers in organic solvents, where k_p is more or less insensitive toward solvent type and monomer concentration.⁹

The variation of k_p for methacrylic acid (MAA) in aqueous solution has been studied in great detail as a function of monomer concentration and of degree of ionization.^{1,2} It appeared interesting to check whether termination in aqueous solution is affected to a similarly large extent as propagation. The termination rate coefficient, k_t , of MAA in aqueous solution has been measured by the single pulse—pulsed laser polymerization—near-infrared (SP-PLP-NIR) technique¹⁰ at 50 °C and 2000 bar for two MAA concentrations, 30 and 60 wt %, and up to monomer conversions of about 90%. Within the SP-PLP-NIR experiment, monomer concentration, c_M , is measured via time-resolved NIR spectroscopy after firing a laser pulse at $t = 0$. These measurements have been carried out at high pressure, as propagation rate is enhanced and termination rate is slowed down, which results in improved signal-to-noise quality. The method provides averaged $\langle k_t \rangle$ values as a function of monomer-to-polymer conversion. It should however be noted that $\langle k_t \rangle$ values from PLP experiments are no chain-length-averaged numbers in the strict sense but should be understood as time-averaged numbers referring to PLP. Termination in MAA polymerization

at 50 °C has also been investigated under stationary conditions with radicals being produced by thermal decomposition of chemical initiators.¹⁰ This method delivers chain-length-averaged $\langle k_t \rangle$.

Within the present study, the SP-PLP-EPR method has been applied to the measurement of termination for MAA polymerization in aqueous solution. This recently developed method combines the advantages of radical concentration being instantaneously produced by a single laser pulse and being monitored by microsecond time-resolved electron paramagnetic resonance (EPR).¹¹ The sensitivity of SP-PLP-EPR is sufficiently high to allow for accurate k_t measurements even at ambient pressure. Because of the direct detection of radical concentration as a function of time t after applying the laser pulse, $c_R(t)$, termination kinetics are far more directly accessed as compared to SP-PLP-NIR, where monomer concentration as a function of t , $c_M(t)$, is measured. Radicals produced by laser-induced photoinitiator decomposition propagate with frequency $k_p c_M$. Radical production occurs at the very moment, when the laser hits the sample. Thus, the chain length, i , of propagating radicals exhibits a very narrow distribution and, unless chain transfer comes into play, increases linearly with time t after applying the laser pulse at $t = 0$; i.e., $i = k_p c_M t + 1$. As a consequence, termination in SP-PLP-EPR occurs between radicals of identical size (as in SP-PLP-NIR and up to a time t from which on chain transfer may no longer be ignored). The SP-PLP-EPR technique thus allows for deducing rate coefficients for termination of two radicals of identical size, $k_t^{i,i}$.

Termination is diffusion controlled from the early stages of the polymerization on. Because of the decrease of diffusion coefficient with molecular size, the termination rate coefficient is lowered toward higher chain length. The composite model¹²

Received: November 2, 2010

Revised: January 5, 2011

Published: February 14, 2011

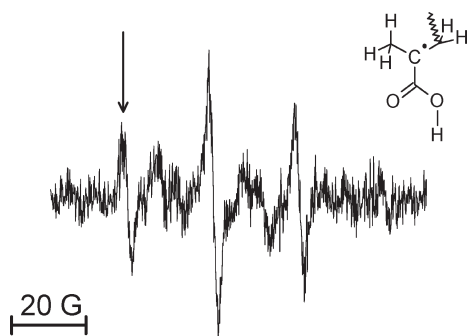


Figure 1. EPR spectrum recorded during pulsed laser polymerization of MAA (10 wt % in water) at 25 °C. The arrow indicates the field position at which signal intensity vs time traces after applying a single laser pulse were recorded during SP-PLP-EPR experiments.

provides an adequate representation of $k_t^{i,i}$, where $k_t^{1,1}$ refers to termination of two radicals both of chain length unity (eq 1).

$$\begin{aligned} k_t^{i,i} &= k_t^{1,1} i^{-\alpha_s} & i \leq i_c \\ k_t^{i,i} &= k_t^{1,1} i^{-\alpha_s + \alpha_i} i^{-\alpha_i} = k_t^0 i^{-\alpha_i} & i > i_c \end{aligned} \quad (1)$$

The model assumes two regimes with distinctly different chain-length dependence. For short radicals, $k_t^{i,i}$ strongly decreases with i . The associated power-law exponent, α_s , is in the range 0.50–1.0. For radicals with sizes above a crossover chain length, i_c , which is typically in the range 30–100, the decay of $k_t^{i,i}$ with chain length is less pronounced. The power-law exponent for these long-chain radicals, α_i , is in the range 0.16–0.24.¹³

So far, SP-PLP-EPR studies into $k_t^{i,i}$ have mostly been carried out for methacrylate-type monomers.^{14–20} EPR measurements in aqueous solution are more difficult due to the dielectric loss of microwave radiation. This problem may be overcome by using specially designed EPR flat cells. The present paper reports the first SP-PLP-EPR data for radical polymerization in aqueous solution. The measurements have been extended to situations of higher conversion, which are mimicked by premixing different amounts of poly(MAA) into the aqueous solution of monomer and photoinitiator. By this strategy, solutions of identical MAA-to-water content, which are associated with identical propagation rate coefficient, may be prepared for different accurately known polymer concentrations.

EXPERIMENTAL SECTION

The SP-PLP-EPR setup has already been detailed.^{11,17} A Bruker Elexsys E 500 series CW-EPR spectrometer was used for the experiments. Typical EPR parameter settings were 3 G field modulation amplitude, 100 kHz field modulation frequency, 20 mW microwave power, and a time constant of 0.01 ms. No saturation of the EPR signals occurs. Flat cells containing sample volumes of 0.15 mL were fitted into the EPR resonator cavity. Irradiation occurred through a grid by a COMPex 102 excimer laser (Lambda Physik) operated on the XeF line (351 nm) at laser energies between 10 and 80 mJ/pulse. The EPR spectrometer and the laser were synchronized by a pulse generator (Scientific Instruments 9314). Temperature control was achieved via an ER 4131VT unit (Bruker) by purging the sample cavity with nitrogen.

Kinematic viscosity, ν , was measured via calibrated KPG Ubbelohde microviscosimeters (Schott GmbH) and corrected via the Hagenbach–Couette procedure. The density of aqueous monomer solutions as a function of temperature, $\rho(T)$, was measured via a DMA 60 instrument (Anton Paar) and used for estimates of dynamic viscosity, η , via $\eta = \nu/\rho$.

Methacrylic acid (MAA) (99%, stabilized with hydroquinone monomethyl ether, Aldrich) was purified by distillation. Poly(methacrylic acid), poly(MAA), $M_w = 370\,000 \text{ g mol}^{-1}$, Polysciences), was used without further purification. Demineralized water was used for preparation of the sample solutions. The photoinitiator 2-hydroxy-2-methylpropiophenone (Darocur, 98%, Aldrich) was used as received at initial concentrations of about $1.6 \times 10^{-2} \text{ mol L}^{-1}$.

A typical experiment starts by measuring the full EPR spectrum under pulse-periodic (20 Hz) laser initiation. This spectrum is measured with a short sweep time of 10 s to avoid significant monomer conversion. The so-obtained spectrum (Figure 1) consists of 13 lines showing the typical pattern of EPR spectra recorded during methacrylate polymerizations.^{17,21} The spectrum of the MAA radical is almost identical to the one of the butyl methacrylate radical.

From the full spectrum, the magnetic field position of the intense line (see arrow in Figure 1) used for the time-resolved EPR measurement is determined. Within the subsequent SP-PLP-EPR experiment, up to 100 individual time traces were co-added to improve signal-to-noise quality. It was checked that the curvature of the EPR intensity vs time traces did not change within each series of co-added traces. Monomer-to-polymer conversion, in the experiments without premixed polymer, was determined gravimetrically and found to be always below 10%. Absolute radical concentration, as required for the kinetic analysis of the time-dependent EPR signals, was obtained by using the calibration procedure detailed elsewhere.¹⁷

RESULTS AND DISCUSSION

Data Treatment. Termination rate coefficients referring to the rate law (eq 2) are determined by fitting time-resolved radical concentration vs time data, $c_R(t)$, from SP-PLP-EPR to eqs 3 and 4.

$$\frac{dc_R}{dt} = -2k_t c_R^2 \quad (2)$$

Under the assumption that k_t is adequately represented by a single, chain-length-averaged value, denoted as $\langle k_t \rangle$, integration of eq 2 yields eq 3, with c_R^0 being the initial (maximum) radical concentration produced by the laser pulse at $t = 0$.

$$\frac{c_R^0}{c_R(t)} = 1 + 2\langle k_t \rangle c_R^0 t \quad (3)$$

To account for chain-length-dependent termination, the composite-model expression for $k_t^{i,i}$ (eq 1) was implemented into eq 2. Integration for the regime of short radicals, i.e., at sizes below the crossover chain length, $i < i_c$, and using the correlation of chain length with time t after applying the laser pulse, $i = k_p c_M t + 1$, yields

$$\frac{c_R^0}{c_R(t)} - 1 = \frac{2k_t^{1,1} c_R^0 ((k_p c_M t + 1)^{1-\alpha_s} - 1)}{k_p c_M (1 - \alpha_s)} \quad 1 \leq i < i_c \quad (4)$$

where c_M is actual monomer concentration. The k_p values for initial MAA concentrations of 10 wt % were taken from ref 2 and were corrected for the mean value of monomer conversion reached in a particular experiment. For chain lengths above i_c , the noise of the measured c_R vs t traces was too large to deduce reliable composite-model parameters. The fitting to eq 4 was carried out for $1 \leq i \leq 100$ with the upper limit being the crossover chain length with methyl methacrylate polymerization.^{18,22} The numbers obtained for $k_t^{1,1}$ and α_s from fitting to eq 4 turned out to be almost insensitive to varying the crossover chain length, i_c .

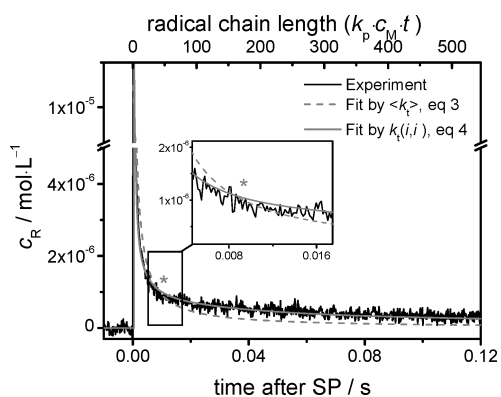


Figure 2. Radical concentration vs time trace for MAA polymerization (10 wt % monomer in aqueous solution) at 10 °C fitted to either eq 3, i.e., assuming a mean value of termination rate coefficient, $\langle k_t \rangle$ (dashed line), or to eq 4, which is based on chain-length-dependent termination with rate coefficients $k_t^{i,i}$ (full line). The asterisk symbol indicates the point of intersection of the fits to eqs 3 and 4.

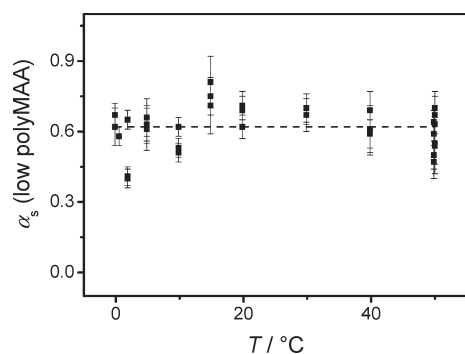


Figure 3. Composite-model parameters $\alpha_s(\text{low polyMAA})$ for termination in aqueous-phase MAA (10 wt %) polymerization; data from fitting measured $c_R(t)$ to eq 4. The dashed line represents the arithmetic mean value of $\alpha_s = 0.62$.

by ± 30 monomer units. The i_c value for MAA may be larger than for MMA due to the action of hydrogen bonds that result in higher chain stiffness, as is indicated by the higher glass-transition temperature of poly(MAA),²³ but there is no clear indication for such an effect. Investigations carried out into chain-length-dependent acrylate and methacrylate termination kinetics so far indicate that higher glass transition temperature is associated with larger i_c .¹⁷

Chain-length-averaged termination rate coefficients, $\langle k_t \rangle$, were obtained by fitting, to eq 3, the c_R vs t traces for MAA polymerization (10 wt % MAA in aqueous solution). The initial radical concentration, c_R^0 , is identified with the highest concentration of radicals produced by monomer addition to a photo-initiator fragment. The c_R^0 values were determined for $t = 0$ from the individual radical concentration vs time traces, which were co-added and then fitted. The time interval covered in the fitting to eq 3 extends up to chain lengths of about 500. Comparison of experimental and fitted curves for 10 wt % MAA at 10 °C clearly demonstrates (see Figure 2) the superior quality of fits to eq 4 and thus the occurrence of chain-length-dependent k_t . As a consequence, in what follows, eq 4 will be used for fitting of the SP-PLP-EPR data.

Results. Plotted in Figure 3 is the composite model parameter for termination of short-chain radicals at low degrees of monomer conversion, $\alpha_s(\text{low polyMAA})$, for polymerizations of

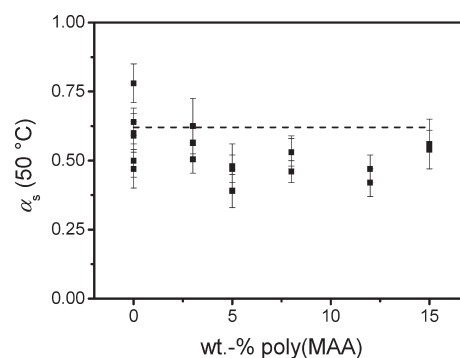


Figure 4. Composite-model parameter α_s for termination in MAA polymerizations (10 wt % in aqueous solution) at 50 °C and different amounts of added poly(MAA). The values are from fitting experimental $c_R(t)$ to eq 4. The dashed line represents $\alpha_s = 0.62$, which is the mean value of the low-conversion data measured between 0 and 50 °C (see Figure 3).

MAA (10 wt %) in aqueous solution at temperatures between 0 and 50 °C. The numbers have been deduced from fits of $c_R(t)$ to eq 4.

The power-law exponent for short-chain radicals, α_s , appears to be insensitive toward temperature, at least in the temperature range under investigation. The arithmetic mean value, $\alpha_s = 0.62$, is indicated by the dashed line. The error associated with the fitting procedure is ± 0.06 . The absolute error of the α_s data from independent experiments should not exceed ± 0.12 . The resulting value for low conversion, $\alpha_s(\text{low polyMAA}) = 0.62 \pm 0.12$, fully agrees with the chain-length dependence predicted from diffusion coefficient data for short radicals, $i < i_c$. With excluded volume effects being taken into account,²⁴ the resulting expression reads $D^i \propto i^{-0.6}$, suggesting a power-law exponent of $\alpha_s = 0.6$ for chain-length-dependent termination.

Moreover, the α_s value for MAA is in close agreement with the power-law exponent for methyl methacrylate (MMA) at low degrees of monomer conversion, as measured by SP-PLP-EPR: $\alpha_s = 0.63$ for bulk polymerization¹⁸ and $\alpha_s = 0.66$ for polymerization in ionic liquid solution.²⁰ The α_s values for other alkyl methacrylates are also of very similar size: 0.65 for *n*-butyl methacrylate,¹⁷ 0.56 for *tert*-butyl methacrylate,¹⁷ and 0.65 for dodecyl methacrylate.¹⁶ Methacrylates with cyclic side chains appear to exhibit slightly lower α_s : 0.50 for both benzyl methacrylate¹⁶ and cyclohexyl methacrylate.¹⁶

At 50 °C, SP-PLP-EPR experiments were performed up to higher conversions. To facilitate comparison of the results, monomer conversion was artificially produced by premixing different amounts of poly(MAA) to 1.25 M aqueous MAA solutions. At identical MAA-to-water content the same k_p applies for the entire set of experiments.² Poly(MAA) was added such as to reach polymer contents of 3, 5, 8, 12, and 15 wt %.

The $c_R(t)$ traces were again analyzed by fitting to eq 4. The resulting α_s values are plotted in Figure 4. The α_s values with premixed poly(MAA) appear to be slightly below $\alpha_s(\text{low polyMAA})$, although this effect occurs within the limits of experimental accuracy and thus cannot be safely established.

Within the SP-PLP-EPR experiments on benzyl methacrylate, cyclohexyl methacrylate, and dodecyl methacrylate up to 25% monomer conversion, no indication of any dependence of α_s on monomer conversion could be detected.¹⁶ In these earlier studies, monomer conversion was induced by laser-induced polymerization, which results in the formation of polymethacrylates of lower

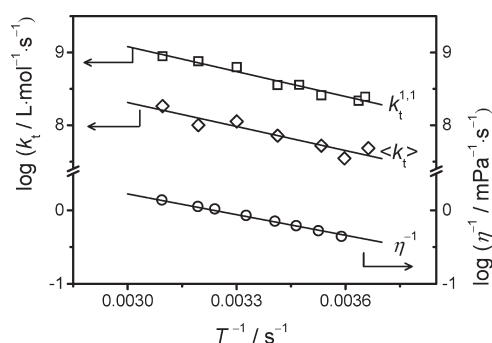


Figure 5. Arrhenius plots of the termination rate coefficients $k_t^{1,1}$ (squares) and $\langle k_t \rangle$ (triangles) for polymerization of MAA (10 wt %) in aqueous solution at low degrees of monomer conversion. The fluidity of the mixture prior to polymerization is represented by reciprocal bulk viscosity, η^{-1} (circles).

molecular mass. The addition of high-molecular-mass polymer, as in the current study, should result in more pronounced effects on α_s , if there are any. The changes indicated in Figure 4 are too small to serve as a clear indication of α_s varying with polymer content.

Pulsed-field-gradient NMR has been used to measure the chain-length dependence of the center-of-mass diffusion coefficient D_i of styrene monomers, dimers, and pentamers as a function of polystyrene concentration in solution of benzene.²⁵ The power-law dependence of the diffusion coefficient at different degrees of monomer conversion, x , has been determined to be $D_i^{1/x} \propto i^{-(\alpha_s(0)+1.75x)}$. Under the assumption that termination rate and diffusion coefficient are proportional to each other, this correlation would indicate that α_s increases with monomer conversion. This is not what our experiments suggest. Perhaps, the range of polymer contents covered in our experiments is not sufficiently high to show a clear effect.

The second parameter from fitting experimental $c_R(t)$ to eq 4 is the rate coefficient for termination of two radicals of chain length unity, $k_t^{1,1}$. Again, the low-conversion region will be studied first. The $k_t^{1,1}$ values for temperatures between 0 and 50 °C are plotted in Figure 5. Included in this figure (as triangles) are chain-length-averaged termination rate coefficients, $\langle k_t \rangle$, deduced from fitting the $c_R(t)$ traces to eq 3. Each $k_t^{1,1}$ and $\langle k_t \rangle$ data point is the arithmetic mean value of up to five individual time-resolved experiments.

The Arrhenius expressions for the two types of termination rate coefficients in Figure 4 read $k_t^{1,1} = 3.27 \times 10^{12} \exp(-2.64 \times 10^3/(K/T)) \text{ L mol}^{-1} \text{ s}^{-1}$ and $\langle k_t \rangle = 4.17 \times 10^{11} \exp(-2.25 \times 10^3/(K/T)) \text{ L mol}^{-1} \text{ s}^{-1}$ with activation energies: $E_A(k_t^{1,1}) = 21.9 \pm 1.5 \text{ kJ mol}^{-1}$ and $E_A(\langle k_t \rangle) = 21.1 \pm 1.5 \text{ kJ mol}^{-1}$, respectively.

Absolute $k_t^{1,1}$ exceeds $\langle k_t \rangle$ by about 1 order of magnitude, which is due to the fact that $k_t^{1,1}$ refers to the largest possible rate coefficient, the one for termination of two radicals of chain length unity, whereas $\langle k_t \rangle$ represents an average value that includes termination of two radicals which may both be fairly large. Via the power-law exponent α_s , the difference between $k_t^{1,1}$ and $\langle k_t \rangle$ may be assigned to $\langle k_t \rangle$ referring to a $k_t^{i,i}$ value for termination of two radicals both of chain length $i = 45$. As can be seen from the asterisk symbol in Figure 2, the curve fitted to eq 4 intersects the curve fitted to eq 3 at $t = 0.010 \text{ s}$. It is this time interval of 0.01 s which a radical in aqueous solution of MAA (10 wt %) at 10 °C requires to grow from chain length unity to chain length 45.

The similarity of the two activation energies, $E_A(k_t^{1,1})$ and $E_A(\langle k_t \rangle)$, may be due to the fact that both the diffusive motion of

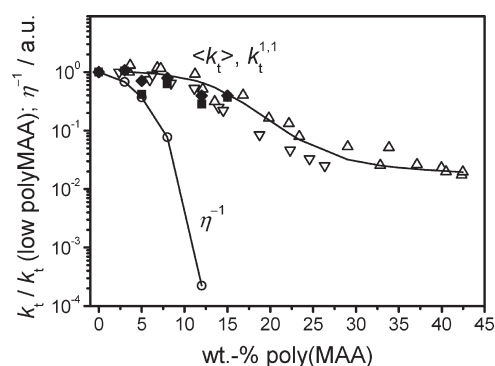


Figure 6. Termination rate coefficients $k_t^{1,1}$ (full squares) and $\langle k_t \rangle_{\text{EPR}}$ (full diamonds) for MAA polymerization (10 wt %) in aqueous solution with premixed poly(MAA) at ambient pressure and 50 °C. The triangles refer to $\langle k_t \rangle_{\text{NIR}}$ from SP-PLP-NIR, as deduced from experiments at 2000 bar and 50 °C¹⁰ on aqueous MAA solutions containing 30 and 60 wt % MAA (triangle and upside-down triangle symbols, respectively). The η^{-1} values (circles) represent the measured fluidity at ambient pressure and 50 °C. The rate coefficients and fluidities are given relative to the associated value at zero polymer content.

small radicals and the segmental diffusion of larger entangled radical chains (that contribute to $\langle k_t \rangle$) experience diffusion control by the friction of the solvent medium, i.e., by the viscosity of the monomer–solvent mixture. Bulk viscosity, to which polymer molecules contribute, does not affect termination at low conversion, as is also indicated by the occurrence of the plateau regions of constant $\langle k_t \rangle$ over an extended conversion range in which bulk viscosity largely increases.

Under center-of-mass diffusion control of $k_t^{1,1}$, the mutual diffusion coefficient, $D_{1,1}$, as given by the Stokes–Einstein relation (eq 5), should allow for correlating $k_t^{1,1}$ with fluidity, η^{-1} , and with hydrodynamic radius (or monomer size), $r_{1,1}$:

$$D_{1,1} = \frac{k_B T}{6\pi r_{1,1} \eta} \quad (5)$$

where k_B is the Boltzmann constant. Equation 5 suggests that $E_A(k_t^{1,1})$ should be close to $E_A(\eta^{-1})$, as has been verified within previous SP-PLP-EPR studies into butyl acrylate²⁶ and into several methacrylate^{17,18} polymerizations in organic phase, where both $E_A(k_t^{1,1})$ and $E_A(\eta^{-1})$ were found to be close to 10 kJ mol⁻¹. The Arrhenius plot for η^{-1} (circles in Figure 4) indicates that also with MAA polymerization in aqueous solution the activation energy of fluidity, $E_A(\eta^{-1}) = 17.9 \pm 2 \text{ kJ mol}^{-1}$, is close to $E_A(k_t^{1,1})$.

The fairly large activation energies of $\langle k_t \rangle$ and of $k_t^{1,1}$ are primarily due to the pronounced temperature dependence of viscosity. As a consequence, the activation energy of termination is even above the one of propagation for MAA polymerization in aqueous solution: $E_A(k_p) = 16.1 \text{ kJ mol}^{-1}$. In an organic environment, $E_A(k_p)$ is mostly above $E_A(k_t)$, as the activation energy of viscosity is rather low for organic solvents including typical monomers.

The $\langle k_t \rangle$ and $k_t^{1,1}$ values, as deduced from $c_R(t)$ traces measured in the presence of premixed poly(MAA), are plotted in Figure 6. In addition to $\langle k_t \rangle$ from SP-PLP-EPR, chain-length-averaged $\langle k_t \rangle_{\text{NIR}}$ from SP-PLP-NIR is included in Figure 6. The SP-PLP-NIR experiments were performed at 2000 bar and 50 °C on aqueous solutions with initial MAA contents of 30 and 60 wt %, respectively. Within the SP-PLP-NIR experiments, poly(MAA)

was not added, but was produced by successive laser pulsing during the experiment. It is gratifying to note that premixing polymer and producing polymer by laser pulsing yields more or less the same type of termination behavior. In order to avoid extrapolation of k_t data measured at different pressures and monomer concentrations to a common reference condition, relative values of $k_t^{1,1}$, $\langle k_t \rangle_{\text{EPR}}$, and $\langle k_t \rangle_{\text{NIR}}$ with respect to the associated limiting value for zero polymer content (or zero conversion) are plotted in Figure 6. The reduced values should adequately reflect the variation of the quantity under consideration with polymer content. Also included in Figure 6 is the inverse of overall viscosity, i.e., the fluidity, η^{-1} , as measured at 50 °C and ambient pressure on aqueous MAA solutions to which different amounts of poly(MAA) have been added. Fluidity is also given on a reduced scale.

The termination rate coefficient vs weight percentage polymer data in Figure 6 demonstrate the closely similar behavior of $k_t^{1,1}$, $\langle k_t \rangle_{\text{EPR}}$, and $\langle k_t \rangle_{\text{NIR}}$. After an initial plateau region, which extends up to about 10 wt % poly(MAA), the termination rate coefficient decreases by about a factor of 5 up to 15 wt % polymer. Reduced bulk fluidity, $\eta^{-1}/\eta^{-1}(0\% \text{ polymer})$, decreases to a much larger extent, by about a factor of 20 000 up to 15 wt % poly(MAA). Moreover, the reduction in fluidity occurs from the very beginning on, and no plateau-type behavior is seen at low degrees of monomer conversion.

In absolute, the $\langle k_t \rangle$ plateau values deduced from SP-PLP-EPR exceed the ones from SP-PLP-NIR by about 1 order of magnitude. This difference primarily results from changes in viscosity by applying 2000 bar and by using higher MAA-in-water concentrations with the SP-PLP-NIR experiments. The higher MAA concentrations chosen for the SP-PLP-NIR experiments are associated with larger mean values of macroradical size, which result in a further lowering of $\langle k_t \rangle$ as a consequence of chain-length-dependent k_t .

The data in Figure 6 demonstrate that eq 5 provides no satisfactory description of either $k_t^{1,1}$ or $\langle k_t \rangle$ over the MAA conversion range up to 15%, as neither $k_t^{1,1}\eta$ nor $\langle k_t \rangle\eta$ remains constant over this conversion range.

This finding comes as no surprise. It is known from the frequently observed plateau regions of constant k_t at low and moderate degrees of monomer conversion that bulk viscosity is not controlling termination rate in this initial polymerization period. It is essentially monomer viscosity or, in the case of solution polymerization, the viscosity of the monomer–solvent mixture which controls termination. That this type of control operates on both small and large radicals, as is indicated by the almost identical conversion dependence of $k_t^{1,1}$ and $\langle k_t \rangle$, may be understood by both translational diffusion of small radicals and segmental reorientation of entangled larger radicals experiencing the friction brought upon by the monomer–solvent mixture, but not by polymeric species.

Measures which change the viscosity of the monomer–solvent mixture, e.g., by varying temperature, pressure, or the type of solvent, affect the termination rate coefficient, as has been demonstrated in SP-PLP-EPR studies by temperature variation^{17,18,26} or by changing the solvent.²⁰ Changing pressure in styrene homopolymerization²⁷ varies the termination rate coefficient for the early plateau region to the same extent as the inverse of monomer viscosity changes. According to these arguments, the initial plateau-type behavior of termination rate coefficients holds as long as a sufficiently large fraction of radicals may diffuse through the monomer–solvent medium and may avoid penetration of

macromolecular coils. Once the fraction of such radicals becomes too small, the termination rate coefficient decreases. This is indicated by the weak decay in termination rate coefficient for MAA (10 wt %) polymerization in aqueous solution above 10% conversion (polymer content).

As is known from polymerization in aqueous solution of 30 and 60 wt % MAA, the decrease in $\langle k_t \rangle$ becomes rather pronounced after passing the initial range of low and moderate conversion. The region where $\langle k_t \rangle$ strongly decreases is assigned to translation-diffusion control. At even higher polymer contents, e.g., above 30 wt % poly(MAA), termination runs into reaction diffusion control, which is associated with a weaker decay of termination rate coefficient upon further enhancement of monomer conversion. It appears to be a matter of priority to extend the SP-PLP-EPR studies into the translation-diffusion and reaction-diffusion controlled regimes and to check whether the chain-length range in which short-chain behavior applies varies with the type of diffusion control.

Our $k_t^{1,1}$ and α_s parameters may be correlated with pulse-gradient NMR and dynamic light scattering data on the diffusion coefficient of monomeric and oligomeric probe molecules in solution of high-molecular-mass polymer coils.^{25,28–30} For diffusion of polyisobutylene molecules in semidilute solution of polyisobutylene in chloroform, Brown and Zhou reported²⁸ that in the case of $M_{\text{probe}} \ll M_{\text{matrix}}$ the product $D_{\text{probe}}\eta_{\text{bulk}}$ increases significantly with weight fraction of the matrix polymer, which is not in line with Stokes–Einstein diffusion (eq 5). The authors conclude that for diffusing molecules of sizes as or below the one of the mesh size of the polymeric matrix the enormous increase in macroscopic viscosity by adding polymer is not accompanied by a corresponding retardation in diffusion of the probe molecules. However, for the inverse condition, $M_{\text{probe}} \gg M_{\text{matrix}}$, the product $D_{\text{probe}}\eta_{\text{bulk}}$ stays constant upon the addition of matrix polymer, in accordance with the Stokes–Einstein relation (eq 5). These findings are consistent with our observations on the product $k_t^{1,1}\eta(T)$: In the initial low-conversion region, macroradicals primarily diffuse through the mixture made up of small monomer and solvent molecules (Figure 5 and ref 11). Under such $M_{\text{probe}} \gg M_{\text{matrix}}$ conditions, the product $k_t^{1,1}\eta$ stays constant when η is identified with the viscosity of the monomer–solvent mixture, but the product $k_t^{1,1}\eta$ is significantly enhanced once η is considered to be the bulk viscosity, as is demonstrated by Figure 6.

The diffusion coefficients of low-molecular-mass species have been reported to decrease by less than a factor of 5 in polymer solutions up to 20 wt % polystyrene^{25,30,31} and up to 30 wt % poly(MMA),²⁹ irrespective of matrix molecular mass. This result from the diffusion studies also fits to the observations from our k_t studies.

The weak decay of both $k_t^{1,1}$ and $\langle k_t \rangle$ from about 10 wt % polymer on (Figure 6) indicates that translational diffusion of polymeric species through the monomer–solvent mixture starts to become restricted by getting entangled with polymeric coils. Toward even higher poly(MAA) contents, as is known from the data in ref 10, termination rate will significantly decrease upon further conversion and may approach the behavior of η^{-1} . The changes of k_t with polymer content will however be less dramatic than the ones of η^{-1} , as low-molecular-mass radicals will be present which diffuse more rapidly. Toward very high degrees of monomer conversion, where diffusion through polymer-free regions of the monomer–solvent mixture essentially ceases, termination may still occur at a faster rate than is indicated by

η^{-1} . Termination under such conditions may occur via reaction diffusion which proceeds fairly rapidly even under conditions of vanishing center-of-mass mobility. Termination at high conversion, where reaction diffusion control operates, is easier to be described than termination at intermediate conversion, where entanglement of diffusing radicals with polymer coils must be considered. As a consequence, the sizes (size distributions) of both radicals and polymer molecules from preceding polymerization need to be known and need to be properly taken into account. Termination at such intermediate conditions is dependent on the history of the particular polymerization, e.g., whether reaction conditions had been chosen such as to produce radicals and polymer molecules of small or large size and with either a narrow or a broad molecular mass distribution. Thus, there is still some way to go before a full picture of termination in radical polymerizations up to high conversion will be available. The present study provides extensive information for the early polymerization period, i.e., for the range controlled by segmental diffusion, where center-of-mass diffusion is fast. The transition into the translation-diffusion controlled range, at polymer contents (monomer conversions) above 10 wt %, as well as the transition into the reaction-diffusion controlled range above 30 wt %, are illustrated in Figure 6.

Because of the rapid decay of radical concentration with time after pulsing, the chain-length dependence of k_t^{ii} can not be accurately measured for higher chain length i , as EPR intensity becomes too low. Because of the proven suitability of the composite model, the chain-length dependence of k_t^{ii} over the full range of i may be estimated by using the $k_t^{1,1}$ and α_s values from the present study for chain lengths below the crossover chain length, which may be adopted from MMA to be $i_c = 100$. The variation of k_t^{ii} at chain lengths above i_c should be given, to a good approximation, by the theoretical power-law exponent, $\alpha_i = 0.16$, which affords for an adequate representation of long-chain termination behavior with the monomer systems studied so far. The measured values together with the adopted numbers for i_c and α_i should provide a reliable and detailed description of the termination kinetics at low and moderate degrees of monomer conversion.

CONCLUSION

Termination in radical polymerization of 10 wt % methacrylic acid in aqueous solution has been investigated via the SP-PLP-EPR method over an extended temperature range with particular emphasis on the chain-length dependence of short radicals at low degrees of monomer conversion. The studies were extended to situations of higher monomer concentrations by addition of poly(MAA). The termination rate coefficient k_t^{ii} of short radicals strongly decreases with chain length i but is almost insensitive toward polymer content up to 10 wt %. The termination rate coefficient decreases with polymer content, but to a much weaker extent than does bulk viscosity.

AUTHOR INFORMATION

Corresponding Author

*E-mail mbuback@gwdg.de; Fax +49 551 393144.

ACKNOWLEDGMENT

A fellowship from the Fonds der Chemischen Industrie (to J.B.) and financial support by the BASF SE are gratefully acknowledged. The authors are grateful to Prof. F. Meyer (Institute for Inorganic

Chemistry, University of Göttingen) for providing the opportunity of using the EPR spectrometer in his laboratory.

REFERENCES

- (1) Lacik, I.; Ucnova, L.; Kukuckova, S.; Buback, M.; Hesse, P.; Beuermann, S. *Macromolecules* **2009**, *42*, 7753–7761.
- (2) Beuermann, S.; Buback, M.; Hesse, P.; Lacik, I. *Macromolecules* **2006**, *39*, 184–193.
- (3) Beuermann, S.; Buback, M.; Hesse, P.; Junkers, T.; Lacik, I. *Macromolecules* **2006**, *39*, 509–516.
- (4) Kuchta, F. D.; van Herk, A. M.; German, A. L. *Macromolecules* **2000**, *33*, 3641–3649.
- (5) Ganachaud, F.; Balic, R.; Monteiro, M. J.; Gilbert, R. G. *Macromolecules* **2000**, *33*, 8589–8596.
- (6) Seabrook, S. A.; Tonge, M. P.; Gilbert, R. G. *J. Polym. Sci., Polym. Chem.* **2005**, *43*, 1357–1368.
- (7) Stach, M.; Lacik, I.; Chorvat, D.; Buback, M.; Hesse, P.; Hutchinson, R. A.; Tang, L. *Macromolecules* **2008**, *41*, 5174–5185.
- (8) Beuermann, S.; Buback, M.; Davis, T. P.; Gilbert, R. G.; Hutchinson, R. A.; Olaj, O. F.; Russell, G. T.; Schweer, J.; van Herk, A. M. *Macromol. Chem. Phys.* **1997**, *198*, 1545–1560.
- (9) Beuermann, S. *Macromol. Rapid Commun.* **2009**, *30*, 1066–1088.
- (10) Beuermann, S.; Buback, M.; Hesse, P.; Hutchinson, R. A.; Kukuckova, S.; Lacik, I. *Macromolecules* **2008**, *41*, 3513–3520.
- (11) Barth, J.; Buback, M. *Macromol. React. Eng.* **2010**, *4*, 288–301.
- (12) Smith, G. B.; Russell, G. T.; Heuts, J. P. A. *Macromol. Theory Simul.* **2003**, *12*, 299–314.
- (13) Barner-Kowollik, C.; Russell, G. T. *Prog. Polym. Sci.* **2009**, *34*, 1211–1259.
- (14) Buback, M.; Egorov, M.; Junkers, T.; Panchenko, E. *Macromol. Rapid Commun.* **2004**, *25*, 1004–1009.
- (15) Buback, M.; Egorov, M.; Junkers, T.; Panchenko, E. *Macromol. Chem. Phys.* **2005**, *206*, 333–341.
- (16) Buback, M.; Müller, E.; Russell, G. T. *J. Phys. Chem. A* **2006**, *110*, 3222–3230.
- (17) Barth, J.; Buback, M.; Hesse, P.; Sergeeva, T. *Macromolecules* **2009**, *42*, 481–488.
- (18) Barth, J.; Buback, M. *Macromol. Rapid Commun.* **2009**, *30*, 1805–1811.
- (19) Barth, J.; Buback, M.; Hesse, P.; Sergeeva, T. *Macromol. Rapid Commun.* **2009**, *30*, 1969–1974.
- (20) Barth, J.; Buback, M.; Schmidt-Naake, G.; Woecht, I. *Polymer* **2009**, *50*, 5708–5712.
- (21) Kamachi, M. *J. Polym. Sci., Polym. Chem.* **2002**, *40*, 269–285.
- (22) Johnston-Hall, G.; Theis, A.; Monteiro, M. J.; Davis, T. P.; Stenzel, M. H.; Barner-Kowollik, C. *Macromol. Chem. Phys.* **2005**, *206*, 2047–2053.
- (23) Schneider, H. A. *Polymer* **2005**, *46*, 2230–2237.
- (24) Flory, P. J. *Principles of Polymer Chemistry*; Cornell University Press: Ithaca, NY, 1953.
- (25) Piton, M. C.; Gilbert, R. G.; Chapman, B. E.; Kuchel, P. W. *Macromolecules* **1993**, *26*, 4472–4477.
- (26) Barth, J.; Buback, M.; Hesse, P.; Sergeeva, T. *Macromolecules* **2010**, *43*, 4023–4031.
- (27) Buback, M.; Kuchta, F. D. *Macromol. Chem. Phys.* **1997**, *198*, 1455–1480.
- (28) Brown, W.; Zhou, P. *Macromolecules* **1989**, *22*, 4031–4039.
- (29) Faldi, A.; Tirrell, M.; Lodge, T. P.; Von Meerwall, E. *Macromolecules* **1994**, *27*, 4184–4192.
- (30) Chekal, B. P.; Torkelson, J. M. *Macromolecules* **2002**, *35*, 8126–8138.
- (31) Cherdhirankorn, T.; Best, A.; Koynov, K.; Peneva, K.; Muellen, K.; Fytas, G. *J. Phys. Chem. B* **2009**, *113*, 3355–3359.